

Constraints on large scale inhomogeneities from WMAP-5 and SDSS: confrontation with recent observations

Paul Hunt^{1*} and Subir Sarkar²

¹*Institute of Theoretical Physics, Warsaw University, ul Hoża 69, 00-681 Warsaw, POLAND*

²*Rudolf Peierls Centre for Theoretical Physics, University of Oxford, 1 Keble Road, Oxford OX1 3NP, UK*

7 November 2018

ABSTRACT

Measurements of the SNe Ia Hubble diagram which suggest that the universe is accelerating due to the effect of dark energy may be biased because we are located in a 200–300 Mpc underdense ‘void’ which is expanding 20–30% faster than the average rate. With the smaller global Hubble parameter, the WMAP-5 data on cosmic microwave background anisotropies can be fitted without requiring dark energy if there is some excess power in the spectrum of primordial perturbations on 100 Mpc scales. The SDSS data on galaxy clustering can also be fitted if there is a small component of hot dark matter in the form of 0.5 eV mass neutrinos. We show however that if the primordial fluctuations are gaussian, the expected variance of the Hubble parameter and the matter density are far too small to allow such a large local void. Nevertheless many such large voids have been identified in the SDSS LRG survey in a search for the late-ISW effect due to dark energy. The observed CMB temperature decrements imply that they are nearly empty, thus these real voids too are in gross conflict with the concordance Λ CDM model. The recently observed high peculiar velocity flow presents another challenge for the model. Therefore whether a large local void actually exists must be tested through observations and cannot be dismissed *a priori*.

Key words: cosmic microwave background, cosmological parameters, cosmology: theory, dark matter, large-scale structure of Universe

1 INTRODUCTION

The Einstein-de Sitter (E-deS) universe with $\Omega_m = 1$ is the simplest model consistent with the spatial flatness expectation of inflationary cosmology. However, Type Ia supernovae (SNe Ia) at redshift $z \simeq 0.5$ appear $\sim 25\%$ fainter than expected in an E-deS universe (Riess et al. 1998; Perlmutter et al. 1999). Together with measurements of galaxy clustering in the Two-degree Field survey (Efstathiou et al. 2002) and of cosmic microwave background (CMB) anisotropies by the Wilkinson Microwave Anisotropy Probe (WMAP) (Spergel et al. 2003), this has established an accelerating universe with a dominant cosmological constant term (or other form of ‘dark energy’) which presumably reflects the present microphysical vacuum state. This ‘concordance’ Λ CDM cosmology (with $\Omega_\Lambda \simeq 0.7$, $\Omega_m \simeq 0.3$, $h \simeq 0.7$) has passed a number of cosmological tests, including baryonic acoustic oscillations (Eisenstein et al. 2005) and measurements of mass fluctuations from clusters and weak lensing (e.g. Contaldi et al. 2003). Further observations of both SNe Ia (Riess et al.

2004; Astier et al. 2006; Wood-Vasey et al. 2007) and the WMAP 3-year results (Spergel et al. 2007) have continued to firm up the model. However there is no physical basis for this model, in particular there are two fundamental problems with the notion that the universe is dominated by vacuum energy. The first is the notorious fine-tuning problem of vacuum fluctuations in quantum field theory — the energy scale of the cosmological energy density is $\sim 10^{-12}$ GeV, many orders of magnitude below the energy scale of $\sim 10^2$ GeV of the Standard Model of particle physics, not to mention the Planck scale of $\sim 10^{19}$ GeV (see Weinberg 1999). The second is the equally acute coincidence problem: since ρ_Λ/ρ_m evolves as the cube of the cosmic scale factor a , there is no reason to expect it to be of $\mathcal{O}(1)$ *today*, yet this is apparently the case. In fact what is actually inferred from observations is *not* an energy density, just a value of $\mathcal{O}(H_0^2)$ for the otherwise unconstrained Λ term in the Friedmann equation. It has been suggested that this may simply be an artifact of interpreting cosmological data in the (oversimplified) framework of a perfectly homogeneous universe in which $H_0 \sim 10^{-42} \text{ GeV} \sim (10^{28} \text{ cm})^{-1}$ is the *only* scale in the problem (Sarkar 2008).

* E-mail: Paul.Hunt@fuw.edu.pl; s.sarkar@physics.ox.ac.uk

In fact the WMAP results alone do *not* require dark en-

ergy if the assumption of a scale-invariant primordial power spectrum is relaxed. This assumption is worth examining given our present ignorance of the physics behind inflation. We have demonstrated (Hunt & Sarkar 2007) that the temperature angular power spectrum of an E-deS universe with $h \simeq 0.44$ matches the WMAP data well if the primordial power is enhanced by $\sim 30\%$ in the region of the second and third acoustic peaks (corresponding to spatial scales of $k \sim 0.01 - 0.1 h \text{ Mpc}^{-1}$). This alternative model with *no* dark energy actually has a slightly better χ^2 for the fit to WMAP-3 data than the ‘concordance power-law Λ CDM model’ and, inspite of having more parameters, has an *equal* value of the Akaike information criterion used in model selection. Other E-deS models with a broken power-law spectrum (Blanchard et al. 2003) have also been shown to fit the WMAP data. Moreover, an E-deS universe can fit measurements of the galaxy power spectrum if it includes a $\sim 10\%$ component of hot dark matter in the form of massive neutrinos of mass $\sim 0.5 \text{ eV}$ (Hunt & Sarkar 2007; Blanchard et al. 2003). Clearly the main evidence for dark energy comes from the SNe Ia Hubble diagram.

A mechanism that sets $\Lambda = 0$ is arguably more plausible than one which leads to the tiny energy density $\rho_\Lambda \simeq 10^{-47} \text{ GeV}^4$ associated with the concordance cosmology.¹ If Λ is indeed zero then perhaps some effect fools us into wrongly deducing the existence of dark energy by *mimicking* a nonzero cosmological constant. It is natural to connect this effect with inhomogenities since cosmic acceleration and large scale nonlinear structure formation appear to have commenced simultaneously. This approach offers the possibility of solving the cosmological constant problems within the framework of general relativity and keeps the introduction of new physics to a minimum.² Several different ways in which inhomogenities could potentially mimic dark energy have been considered in the literature — for reviews see Celerier (2007); Buchert (2008); Enqvist (2008). In an inhomogeneous universe averaged quantities satisfy modified Friedmann equations which contain extra terms corresponding to ‘backreaction’ since the operations of spatial averaging and time evolution do not commute (Buchert 2000). The backreaction terms depend upon the variance of the local expansion rate and hence increase as inhomogenities develop. Whether backreaction can indeed account for the apparent cosmological acceleration is hotly debated and remains an open question at present (Wetterich 2003; Ishibashi & Wald 2006; Vanderveld et al. 2007; Wiltshire 2007; Khosravi et al. 2007; Leith et al. 2008; Behrend et al. 2008; Rasanen 2008; Paranjpe & Singh 2008).

Another possibility is that inhomogeneities affect light propagation on large scales and cause the luminosity distance-redshift relation to resemble that expected for an accelerating universe. This has been investigated for a ‘Swiss-cheese’ universe in which voids modelled by patches

of Lemaître-Tolman-Bondi (LTB) space-time are distributed throughout a homogenous background. However, the results seem to be model dependent: some authors find the change in light propagation to be negligible because of cancellation effects (Biswas & Notari 2008; Brouzakis et al. 2008; Brouzakis & Tetradis 2008), whereas Marra et al. (2007) claim it can partly mimic dark energy if the voids have radius 250 Mpc (Marra et al. 2008). Mattsson (2007) has noted that observers may preferentially choose sky regions with underdense foregrounds when studying distant objects such as SNe Ia, so the expansion rate along the line-of-sight is then greater than average; such a selection effect he argues can allow an inhomogeneous universe to fit the observations without dark energy.

In this paper we are mainly interested in a ‘local void’ (sometimes referred to as “Hubble bubble”) as an explanation for dark energy; to prevent an excessive CMB dipole moment due to our peculiar velocity we must be located near the centre of the void. An underdense void expands faster than its surroundings, thus younger supernovae inside the void would be observed to be receding more rapidly than older supernovae outside the void. Under the assumption of homogeneity this would lead to the mistaken conclusion that the expansion rate of the Universe is accelerating, although both the void and the global universe are actually decelerating. Henceforth we use the ‘Hubble contrast’ $\delta_H \equiv (H_{\text{in}} - H_{\text{out}})/H_{\text{out}}$ to characterise the void expansion rate, where H_{in} and H_{out} are the Hubble parameters inside and outside the void respectively. (Other authors have used the ‘jump’ $\mathcal{J} \equiv H_{\text{in}}/H_{\text{out}} = 1 + \delta_H$ to characterise the void.) The reduced Hubble parameter h is defined as usual by $H_{\text{out}} = 100h \text{ km s}^{-1} \text{ Mpc}^{-1}$ throughout.

The local void scenario has been investigated by several authors using a variety of methods (Celerier 1999; Tomita 2000, 2001a,b,c; Iguchi et al. 2002; Tomita 2003; Moffat 2005a,b, 2006; Mansouri et al. 2005; Vanderveld et al. 2006; Garfinkle 2006; Chung & Romano 2006; Alnes et al. 2006; Alnes & Amarzguioui 2007; Alexander et al. 2007; Biswas et al. 2007; Caldwell & Stebbins 2008; Clarkson et al. 2008; Uzan et al. 2008; Garcia-Bellido & Haugboelle 2008a; Clifton et al. 2008; Garcia-Bellido & Haugboelle 2008b). In a series of papers, Tomita modelled the void as a open Friedmann-Robertson-Walker (FRW) region joined by a singular mass shell to a FRW background and found that a void with radius 200 Mpc and $\delta_H = 0.25$ fits the supernova Hubble diagram without dark energy (Tomita 2001c). Alnes et al. (2006) showed that a LTB region which reduces to a E-deS cosmology with $h = 0.51$ at a radius of 1.4 Gpc with $\delta_H = 0.27$ can match both the supernova data and the location of the first acoustic peak in the CMB. Alexander et al. (2007) attempted to find the smallest possible void consistent with the current supernova results — their LTB-based ‘minimal void’ model has a radius of 350 Mpc and $\mathcal{J} \simeq 1.2$ i.e. $\delta_H \simeq 0.2$; a void of similiar size but with $\delta_H = 0.3$ had been discussed earlier (Biswas et al. 2007). Unfortunately, since this model is equivalent to an E-deS universe with $h = 0.44$ *outside* the void where the Sloan Digital Sky Survey (SDSS) luminous red galaxies lie, as it stands it is unable to fit the measurements of the baryonic acoustic oscillation (BAO) peak at $z \sim 0.35$ (Blanchard et al. 2006). LTB models of much larger voids

¹ ‘Quintessence’ models, which attempt to address the coincidence problem, also *assume* that every other contribution to the vacuum energy cancels apart from that of the quintessence field.

² In models that seek to explain the observations through modifications of gravity, the relevant scale of H_0^{-1} has to be introduced *by hand*, just as in quintessence models the quintessence field has to be given a mass of order H_0 — these are technically *unnatural* choices since this is an infrared scale for any microphysical theory.

were considered by Garcia-Bellido & Haugboelle (2008a) (with radii of 2.3 Gpc and 2.5 Gpc and Hubble contrasts of 0.18 and 0.30 respectively) and it was demonstrated they can fit the supernova data, BAO data and the location of the first CMB peak. Clifton et al. (2008) found the best fit to the SNe Ia data for a void of radius 1.3 ± 0.2 Gpc and an underdensity of about 70% at the centre and Bolejko & Wyithe (2008) confirmed that such a void provides an excellent fit to the latest ‘Union dataset’ (Kowalski et al. 2008). Moreover Inoue & Silk (2006) have shown that the unexpected alignment of the low multipoles in the CMB anisotropy can be attributed to the existence of a local void of radius $300 h^{-1}$ Mpc. These authors also suggested that the anomalous ‘cold spot’ in the WMAP southern sky is due to a similar void at $z \sim 1$ and some evidence for this has emerged subsequently (Rudnick et al. 2007). Recently, a large number of voids of varying sizes have been identified in the SDSS Luminous Red Galaxy (LRG) catalog in a search for the late integrated Sachs-Wolfe (ISW) effect due to dark energy (Granett et al. 2008b).

How likely is the existence of such huge voids according to standard theories of structure formation? Statistical measures of the void distribution such as the void probability function and underdense probability function have been estimated from the 2dfGRS, SDSS and DEEP2 galaxy redshift surveys (Hoyle & Vogeley 2004; Croton et al. 2004; Patiri et al. 2005; Conroy et al. 2005; Tikhonov 2006; Tinker et al. 2007; Tikhonov 2007; von Benda-Beckmann & Mueller 2007). Void probability statistics have also been examined theoretically using analytical methods (Sheth & van de Weygaert 2004; Furlanetto & Piran 2006; Shandarin et al. 2006) and N-body simulations (Little & Weinberg 1994; Schmidt et al. 2000; Arbabi-Bidgoli & Mueller 2002; Benson et al. 2003; Padilla et al. 2005). However such studies have been restricted to voids with radii of 10-30 Mpc. The scales of the large voids we are considering lie in the linear regime where the variance of the Hubble contrast is directly related to the matter power spectrum $\mathcal{P}_m(k)$. It has been noted (using results from Turner et al. (1992)) that above 100 Mpc linear theory predictions agree well with N-body simulation results, although on smaller scales the Hubble contrast is underestimated due to non-linear effects (Shi et al. 1996). Applying linear theory and using the measured CMB dipole velocity, Wang et al. (1998) obtained the model-independent result $\langle \delta_H \rangle_R^{1/2} < 10.5 h^{-1} \text{Mpc}/R$ in a sphere of radius R . (This ought to be an acceptable procedure up to scales of order $800 h^{-1}$ Mpc — on larger scales, relativistic corrections become increasingly important.) In this paper we update these results by determining the probability distribution of δ_H and the density contrast on various scales using constraints on $\mathcal{P}_m(k)$ from WMAP 5-year data (Komatsu et al. 2008) and the SDSS galaxy power spectrum (Tegmark et al. 2003). We find that even the ‘minimal local void’ is *extremely* unlikely if the primordial density perturbation is indeed gaussian as is usually assumed and the other LTB model voids even less so. However by the same token, the ISW effect due to the voids seen in the SDSS LRG survey (Granett et al. 2008b) appears to be too strong. Moreover, observed large-scale peculiar velocities appear to be much higher than expected (Kashlinsky et al. 2008; Watkins et al.

2008). It would appear that the standard model of structure formation itself needs reexamination hence the existence of a large local void cannot be dismissed on these grounds.

2 MODELS

We study variations of the Hubble parameter in the context of two different cosmological models, both of which fit the WMAP and SDSS data but have different amounts of power on spatial scales of $\mathcal{O}(100)$ Mpc. The intention is to examine whether previous conclusions concerning the magnitude of such variations (Wang et al. 1998) can be circumvented in an unorthodox model.

Our first model is the standard Λ CDM concordance model with a power-law primordial power spectrum. The spectral index and amplitude $\mathcal{P}_{\mathcal{R}}$ of the comoving curvature perturbation spectrum are evaluated at a pivot point of $k = 0.05 \text{Mpc}^{-1}$. The second model is dubbed the ‘CHDM bump model’ since it has both cold and hot dark matter and a ‘bump’ in the primordial spectrum. It was developed by us (Hunt & Sarkar 2007) based upon the supergravity multiple inflation scenario in which ‘flat direction’ fields undergo gauge symmetry-breaking phase transitions during inflation triggered by the fall in temperature (Adams et al. 1997; Hunt & Sarkar 2004). Each flat direction ψ has a gravitational strength coupling to the inflaton ϕ , giving a contribution to the potential of the form $V \subset \frac{1}{2} \lambda \phi^2 \psi^2$. The flat directions are lifted by supergravity corrections and non-renormalisable superpotential terms. Thus when a phase transition occurs the flat direction evolves rapidly from the origin where it was trapped by thermal effects to the global minimum of the potential. Each phase transition changes the effective inflaton mass from m_ϕ^2 to $m_\phi^2 - \lambda \langle \psi \rangle^2$. Since the primordial power spectrum is very sensitive to the inflaton mass this can introduce features into the spectrum. We showed that two flat directions ψ_1 and ψ_2 which cause successive phase transitions about 2 e-folds apart and create a small bump in the power spectrum centred on $k \simeq 0.03 h \text{Mpc}^{-1}$, allow an E-deS model with $h = 0.44$ to fit the WMAP data (Hunt & Sarkar 2007). The effective scalar potential is:

$$V(\phi, \psi_1, \psi_2) = \begin{cases} V_0 - \frac{1}{2} m^2 \phi^2, & t < t_1, \\ V_0 - \frac{1}{2} m^2 \phi^2 - \frac{1}{2} \mu_1^2 \psi_1^2 \\ + \frac{1}{2} \lambda_1 \phi^2 \psi_1^2 + \frac{\gamma_1}{M_{\text{P}}^{n_1-4}} \psi^{n_1}, & t_2 \geq t \geq t_1, \\ V_0 - \frac{1}{2} m^2 \phi^2 - \frac{1}{2} \mu_1^2 \psi_1^2 \\ + \frac{1}{2} \lambda_1 \phi^2 \psi_1^2 + \frac{\gamma_1}{M_{\text{P}}^{n_1-4}} \psi^{n_1} \\ - \frac{1}{2} \mu_2^2 \psi_2^2 - \frac{1}{2} \lambda_2 \phi^2 \psi_2^2 \\ + \frac{\gamma_2}{M_{\text{P}}^{n_2-4}} \psi^{n_2}, & t \geq t_2. \end{cases} \quad (1)$$

Here t_1 and t_2 are the times at which the first and second phase transitions begin, λ_1 and λ_2 are the couplings between ϕ and the flat directions, γ_1 and γ_2 are the co-efficients of the non-renormalisable terms of order n_1 and n_2 , and V_0 is a constant which dominates the potential. In the slow-roll approximation the height of the bump is $\mathcal{P}_{\mathcal{R}}^{(1)}$, and the amplitude of the primordial perturbation spectrum to the left and right of the bump is $\mathcal{P}_{\mathcal{R}}^{(0)}$ and $\mathcal{P}_{\mathcal{R}}^{(2)}$ respectively, where

$$\mathcal{P}_{\mathcal{R}}^{(0)} = \frac{9H^6}{4\pi^2 m^4 \phi_0^2}, \quad (2)$$

$$\mathcal{P}_{\mathcal{R}}^{(1)} = \frac{\mathcal{P}_{\mathcal{R}}^{(0)}}{(1 - \Delta m_1^2)^2}, \quad (3)$$

$$\mathcal{P}_{\mathcal{R}}^{(2)} = \frac{\mathcal{P}_{\mathcal{R}}^{(0)}}{(1 - \Delta m_1^2 + \Delta m_2^2)^2}. \quad (4)$$

Here ϕ_0 is the initial value of ϕ and

$$\Delta m_1^2 = \frac{\lambda_1}{m^2} \left(\frac{\mu_1^2 M_{\text{P}}^{n_1-4}}{n_1 \gamma_1} \right)^{2/(n_1-2)}, \quad (5)$$

$$\Delta m_2^2 = \frac{\lambda_2}{m^2} \left(\frac{\mu_2^2 M_{\text{P}}^{n_2-4}}{n_2 \gamma_2} \right)^{2/(n_2-2)}, \quad (6)$$

are the fractional changes in the inflaton mass-squared due to the phase transitions. The bump lies approximately between the wavenumbers k_1 and k_2 where $k_2 = k_1 e^{H(t_2-t_1)}$. In this paper we set γ_1 and γ_2 equal to unity, $m^2 = 0.005 H^2$, $\phi_0 = 0.01 M_{\text{P}}$, $\mu_1^2 = \mu_2^2 = 3H^2$ and $\lambda_1 = \lambda_2 = H^2/M_{\text{P}}^2$ throughout as in our earlier work (Hunt & Sarkar 2007). In fitting to the WMAP-5 data we also consider continuous (non-integral) values of n_1 and n_2 to determine whether a different shape of the ‘bump’ gives a better fit, keeping in mind that its physical origin may be different from multiple inflation (Chung et al. 1999; Lesgourgues 1999; Kaloper & Kaplinghat 2003; Easther et al. 2001; Wang et al. 2005; Gong 2005; Ashoorian & Krause 2006; Bean et al. 2008).

A pure cold dark matter (CDM) model exhibits excessive galaxy clustering on small scales. Therefore it is necessary to include a hot dark matter (HDM) component which suppresses structure formation below the free-streaming scale. We obtain a good match to the shape of the SDSS galaxy power spectrum with 3 neutrino species of mass ~ 0.5 eV. Hence the CHDM bump model has $\Omega_{\text{b}} \simeq 0.1$, $\Omega_{\nu} \simeq 0.1$, $\Omega_{\text{c}} \simeq 0.8$ (Hunt & Sarkar 2007).

3 THE DATA SETS

We fit to the WMAP 5-year (Nolta et al. 2008) temperature-temperature (TT), temperature-electric polarisation (TE), and electric-electric polarisation (EE) spectra. Compared to the WMAP-3 results, the WMAP-5 measurement of the TT spectrum is $\sim 2.5\%$ higher in the region of the acoustic peaks due to the revised beam transfer functions, and the third acoustic peak is determined more accurately. Polarisation measurements are improved by the use of data from an additional waveband.

We also fit the linear matter power spectrum $\mathcal{P}_{\text{m}}(k)$ to the measurement of the real space galaxy power spectrum $\mathcal{P}_{\text{g}}(k)$ in the SDSS (Tegmark et al. 2003).

4 METHOD

The Hubble contrast δ_H smoothed over a sphere of radius R is (Shi et al. 1996)

$$\delta_H(\mathbf{x})^R = \int d^3\mathbf{y} \frac{\mathbf{v}(\mathbf{y})}{H_{\text{out}}} \cdot \frac{\mathbf{y} - \mathbf{x}}{|\mathbf{y} - \mathbf{x}|^2} W_R(\mathbf{y} - \mathbf{x}), \quad (7)$$

where \mathbf{v} is the peculiar velocity field and W_R is the ‘top hat’ window function,

$$W_R(\mathbf{x}) = \begin{cases} 3/(4\pi R^3), & |\mathbf{x}| \leq R, \\ 0, & |\mathbf{x}| > R. \end{cases} \quad (8)$$

Using linear perturbation theory (Peebles 1993) it can be shown that the variance of δ_H is related to the matter power spectrum as (Wang et al. 1998)

$$\langle \delta_H^2 \rangle_R = \frac{f^2}{2\pi^2} \int_0^\infty dk k^2 \mathcal{P}_{\text{m}}(k) W_H^2(kR). \quad (9)$$

Here the window function W_H is

$$W_H(kR) = \frac{3}{k^3 R^3} \left(\sin kR - \int_0^{kR} dy \frac{\sin y}{y} \right), \quad (10)$$

and the dimensionless linear growth rate f for a Λ CDM universe can be approximated by (Lahav et al. 1991; Hamilton 2001)³

$$f(\Omega_{\text{m}}, \Omega_{\Lambda}) \simeq \Omega_{\text{m}}^{4/7} + \frac{\Omega_{\Lambda}}{70} \left(1 + \frac{\Omega_{\text{m}}}{2} \right). \quad (11)$$

Similarly, the variance of the density contrast $\delta \equiv (\rho_{\text{in}} - \rho_{\text{out}})/\rho_{\text{out}}$ in a sphere of radius R is

$$\langle \delta^2 \rangle_R = \frac{1}{2\pi^2} \int_0^\infty dk k^2 \mathcal{P}_{\text{m}}(k) W^2(kR), \quad (12)$$

where the window function

$$W(kR) = \frac{3}{k^3 R^3} (\sin kR - kR \cos kR), \quad (13)$$

is the Fourier transform of W_R .

The variance of the peculiar velocity is given by

$$\langle v^2 \rangle_R = \frac{f^2 H_{\text{out}}^2}{2\pi^2} \int_0^\infty dk \mathcal{P}_{\text{m}}(k) W^2(kR). \quad (14)$$

Finally we also consider $\Omega_{\text{in}} = 8\pi G \rho_{\text{in}}/H_{\text{in}}^2$, the ratio of the matter density to the critical density as measured locally by an observer inside the void (Wang et al. 1998). The variance of the perturbation $\delta_{\Omega} \equiv (\Omega_{\text{in}} - \Omega_{\text{m}})/\Omega_{\text{m}}$ is then

$$\langle \delta_{\Omega}^2 \rangle_R = \frac{1}{2\pi^2} \int_0^\infty dk k^2 \mathcal{P}_{\text{m}}(k) W_{\Omega}^2(kR), \quad (15)$$

where

$$W_{\Omega}(kR) = \frac{3}{k^3 R^3} \left[(2f - 1) \sin kR + kR \cos kR + 2f \int_0^{kR} dy \frac{\sin y}{y} \right]. \quad (16)$$

We use the Monte Carlo Markov Chain (MCMC) approach to cosmological parameter estimation, which is a method for drawing samples from the posterior distribution $P(\boldsymbol{\varpi}|\text{data})$ of the cosmological parameters $\boldsymbol{\varpi}$, given the data. For a discussion of the MCMC likelihood analysis see Appendix B of Hunt & Sarkar (2007). Given n samples $\boldsymbol{\varpi}^{(i)}$ the best estimate for the distribution is

$$P(\boldsymbol{\varpi}|\text{data}) \simeq \frac{1}{n} \sum_{i=1}^n \delta^D(\boldsymbol{\varpi} - \boldsymbol{\varpi}^{(i)}), \quad (17)$$

³ Hamilton (2001) emphasized that the power-law exponent is $4/7$ for a high density universe, so we have corrected the previous formula from Lahav et al. (1991) accordingly.

where δ^D is the Dirac delta function. The CMB angular power spectrum and the matter power spectrum (corrected for non-linear evolution using the ‘Halofit’ (Smith et al. 2002) procedure) of each model are calculated using a modified version of the CAMB⁴ cosmological Boltzmann code (Lewis et al 2000) following the approach of Hunt & Sarkar (2007). While the temperature of the CMB monopole would be affected if we are located near the centre of a spherically symmetric void, secondary anisotropies due to the void are expected to decay rapidly for higher multipoles (Alexander et al. 2007). We therefore neglect the possible effects of the void on the angular power spectra since these are important only at low multipoles where the cosmic variance is large. The integrals for the variances in eqs.(9, 12-15) were evaluated numerically. Care was taken to ensure the precise values of the integration limits did not affect the results. We compute f numerically using the GROW λ software package (Hamilton 2001). We use a version of the COSMOMC⁵ package (Lewis & Bridle 2002) modified to include $\langle \delta_H^2 \rangle_R^{1/2}$, $\langle \delta^2 \rangle_R^{1/2}$, $\langle v^2 \rangle_R^{1/2}$ and $\langle \delta_\Omega^2 \rangle_R^{1/2}$ for 8 values of R as additional derived parameters determined from the base Monte Carlo parameters. It follows from eq.(17) that 1-D marginalised distributions of these quantities for each R value are obtained by plotting histograms of the samples. The probability distribution $P(\delta_H|\text{data})_R$ of δ_H on the scale R given the data can be written as

$$P(\delta_H|\text{data})_R = \int P(\delta_H|\boldsymbol{\varpi})_R P(\boldsymbol{\varpi}|\text{data}) d\boldsymbol{\varpi}. \quad (18)$$

Using eq.(17) this is approximated by

$$P(\delta_H|\text{data})_R = \frac{1}{n} \sum_{i=1}^n P(\delta_H|\boldsymbol{\varpi}^{(i)})_R, \quad (19)$$

where

$$P(\delta_H|\boldsymbol{\varpi})_R = \frac{1}{\sqrt{2\pi \langle \delta_H^2 \rangle_R}} \exp\left(-\frac{\delta_H^2}{2 \langle \delta_H^2 \rangle_R}\right). \quad (20)$$

We calculate the probability distribution $P(\delta|\text{data})_R$ in same way.

Flat priors are used on the parameters listed in Table 1. Here θ is the ratio of the sound horizon to the angular diameter distance to last scattering (multiplied by 100), τ is the optical depth (due to reionisation) to the last scattering surface, and $f_\nu \equiv \Omega_\nu/\Omega_d$ is the fraction of dark matter in the form of neutrinos, where the total dark matter density is $\Omega_d \equiv \Omega_c + \Omega_\nu$. We assume the chains have converged when the Gelman-Rubin ‘R’ statistic falls below 1.02. We evaluate the sum in eq.(19) when post-processing the chains.

5 RESULTS

The mean values of the marginalised cosmological parameters together with their 68% confidence limits are listed in Table 2. As in our previous work (Hunt & Sarkar 2007) we also list the value of the Akaike information criterion (AIC) relative to the Λ CDM power-law model. Recall that

the AIC is defined as $\text{AIC} \equiv -2 \ln \mathcal{L}_{\text{max}} + 2N$ (Akaike 1974) where \mathcal{L}_{max} is the maximum likelihood and N the number of parameters. It is a commonly used guide for judging whether additional parameters are warranted given the increased model complexity, and quantifies the compromise between improving the fit and adding extra parameters.

The CHDM ‘bump’ model with $n_1 = 12$ and $n_2 = 13$ has a χ^2 equal to the Λ CDM power-law model. Allowing n_1 and n_2 to vary freely further improves the fit to the data with the consequence that the CHDM model with n_1 and n_2 continuous is *favoured* over the Λ CDM model according to the AIC. The primordial power spectrum of the models is shown in Fig.1 together with the fit to the WMAP TT and TE spectra and the SDSS galaxy power spectrum.

The uncertainties of the derived parameters are smaller compared to those derived from the WMAP 3-year results, as would be expected for higher quality data. For example, the optical depth due to reionisation for the CHDM model with continuous n_1 and n_2 has gone from $\tau = 0.075_{-0.012}^{+0.012}$ to $\tau = 0.0771_{-0.0083}^{+0.0073}$ due to the more accurate polarisation measurements. The shape of the ‘bump’ in the primordial power spectrum for the CHDM model with continuous n_1 and n_2 is slightly changed by the new data. Although the quantity $\ln(10^{10} \mathcal{P}_{\mathcal{R}}^{(0)})$ is almost unaltered, $\ln(10^{10} \mathcal{P}_{\mathcal{R}}^{(1)})$ has increased slightly from a 3-year value of $3.429_{-0.049}^{+0.048}$ to a 5-year value of $3.462_{-0.036}^{+0.036}$ because of the increased amplitude of the TT spectrum for multipoles $\ell > 200$. Due to the increased height of the third acoustic peak, $\ln(10^{10} \mathcal{P}_{\mathcal{R}}^{(2)})$ has increased from $3.091_{-0.067}^{+0.071}$ to $3.183_{-0.041}^{+0.043}$ and $10^4 k_2$ fallen from $585_{-82}^{+36} \text{ Mpc}^{-1}$ to $500_{-54}^{+21} \text{ Mpc}^{-1}$. The increased amplitude of the primordial power spectrum on small scales has raised σ_8 from a value of $0.662_{-0.064}^{+0.063}$ to $0.700_{-0.098}^{+0.098}$.

The mean values of the variances $\langle \delta_H^2 \rangle_R$, $\langle \delta^2 \rangle_R$, $\langle v^2 \rangle_R$ and $\langle \delta_\Omega^2 \rangle_R$, together with their 1σ limits, are plotted in Fig.2. The different variances in the two models can be understood with reference to the matter power spectrum. From the relativistic Poisson equation, a given density perturbation leads to a larger curvature perturbation in a higher density universe. Since the amplitude of the primordial curvature perturbation is similar in both models (as can be seen from Fig.1) the density contrast during the early matter dominated era is *greater* in the Λ CDM universe than in the higher density CHDM universe. Although the growth of density perturbations at late times is suppressed in a low density universe, this means that the matter power spectrum of the Λ CDM universe is larger on all scales than that of the CHDM universe, when measured in units of $h^{-3} \text{ Mpc}^3$. (This is not evident in Fig.1 where the *galaxy* power spectrum is shown — the galaxies are more biased in the CHDM universe than in Λ CDM so the matter power spectrum is lower.)

This also explains why, as seen in Fig.2, $\langle \delta^2 \rangle_R$ is uniformly greater for the Λ CDM model. The linear growth factor f is smaller for the Λ CDM universe, and the peak in the matter power spectrum occurs at a larger scale. Thus the quantity $f^2 \mathcal{P}_m(k)$ which appears in eq.(9) is greater for the Λ CDM universe for wavenumbers below $k_{\text{cross}} \simeq 0.01 h \text{ Mpc}^{-1}$ but is greater for the CHDM universe for wavenumbers above k_{cross} . The window function W_H (10) makes $\langle \delta_H^2 \rangle_R$ sensitive to the value of $f^2 \mathcal{P}_m(k)$ for the wavenumber $k \simeq \pi/R$. Consequently the $\langle \delta_H^2 \rangle_R$ curves for the two models cross at the scale $\pi/k_{\text{cross}} \simeq 300 h^{-1} \text{ Mpc}$

⁴ <http://camb.info>

⁵ <http://cosmologist.info/cosmomc/>

Table 1. The priors adopted on the base Monte Carlo parameters of the various models, as well as on the derived parameters: the Hubble constant and the age of the Universe.

Parameter	Model					
	Λ CDM power-law		CHDM bump with $n_1 = 12, n_2 = 13$		CHDM bump with n_1, n_2 continuous	
	Lower limit	Upper limit	Lower limit	Upper limit	Lower limit	Upper limit
$\Omega_b h^2$	0.005	0.1	0.005	0.1	0.005	0.1
$\Omega_c h^2$	0.01	0.99				
θ	0.5	10.0	0.5	10.0	0.5	10.0
τ	0.01	0.8	0.01	0.8	0.01	0.8
f_ν			0.01	0.3	0.01	0.3
n_s	0.5	1.5				
$10^4 k_1 / \text{Mpc}^{-1}$			0.01	600	0.01	600
$10^4 k_2 / \text{Mpc}^{-1}$			0.01	800	0.01	1100
$\ln(10^{10} \mathcal{P}_{\mathcal{R}})$	2.7	4.0				
$\ln(10^{10} \mathcal{P}_{\mathcal{R}}^{(0)})$			2.0	6.0	2.0	6.0
$\ln(10^{10} \mathcal{P}_{\mathcal{R}}^{(1)})$					2.0	6.0
$\ln(10^{10} \mathcal{P}_{\mathcal{R}}^{(2)})$					2.0	6.0
h	0.4	1.0	0.1	1.0	0.1	1.0
Age/Gyr	10.0	20.0	10.0	20.0	10.0	20.0

as seen in Fig.2. The two $\langle v^2 \rangle_R$ curves cross at a smaller scale of about $100 h^{-1} \text{Mpc}$. This is because the integral (14) for the variance in the peculiar velocity $\langle v^2 \rangle_R$ is more strongly weighted towards small wavenumbers than the corresponding expression eq.(9) for the variance in the Hubble contrast $\langle \delta_H^2 \rangle_R$, which has an additional factor of k^2 . Finally for $\langle \delta_\Omega^2 \rangle_R$ the situation is intermediate between that for the variance in the density contrast and the variance in the Hubble contrast, since only some of the terms in W_Ω contain factors of f .

The scale dependence of $\langle \delta_H^2 \rangle_R$ is the reason that the $P(\delta_H | \text{data})_R$ distribution is broader for the Λ CDM power-law and the CHDM ‘bump’ models on scales above and below $300 h^{-1} \text{Mpc}$, respectively, as shown in Fig.3. Similarly the $P(\delta | \text{data})_R$ distribution is broader for the Λ CDM model on all scales, as seen in Fig.4.

To illustrate our findings we calculate the probability of a fluctuation in the Hubble contrast greater than or equal to a given value δ_H^0 in a sphere of radius R , given by:

$$\text{Probability}(\delta_H \geq \delta_H^0)_R = \int_{\delta_H^0}^{\infty} P(\delta_H | \text{data})_R d\delta_H. \quad (21)$$

Since $P(\delta_H | \text{data})_R$ is symmetric this is also equivalent to the probability of a fluctuation being less than or equal to $-\delta_H^0$. As seen in Fig.5, the probability of a large excursion in δ_H is largest on small scales, in accordance with physical intuition. Note that the probability on all scales tends to a value of 1/2 for small δ_H^0 because the fluctuation has an equal probability of being positive or negative. The probability is greater for the CHDM model than for the Λ CDM

model on small scales because the $P(\delta_H | \text{data})_R$ distribution is broader for the CHDM model on these scales. Conversely since the distribution is broader on large scales for the Λ CDM model, the probability is greater there for this model.

Similarly we calculate the probability of a fluctuation in the density contrast less than or equal to a given value $-\delta^0$ in a sphere of radius R , which is given by:

$$\text{Probability}(\delta \leq -\delta^0)_R = \int_{-\infty}^{-\delta^0} P(\delta | \text{data})_R d\delta. \quad (22)$$

This probability is greater for the Λ CDM model on all scales as seen in Fig.6, due to the broader $P(\delta | \text{data})_R$ distribution.

Moreover, we can determine the probability of one or more voids with comoving volume V_1 occurring within some larger comoving volume V_2 . If the ratio V_2/V_1 is N to the nearest integer and p is the probability of a void with volume V_1 , then the probability of n voids within V_2 is $\binom{N}{n} p^n (1-p)^{N-n}$ where $\binom{N}{n}$ is the binomial coefficient. The expected number of voids within V_2 is Np .

6 DISCUSSION

A void with $\delta_H \simeq 0.2 - 0.3$ and a radius exceeding $100 h^{-1} \text{Mpc}$ is required to fit the supernova data without dark energy (Tomita 2001c; Biswas et al. 2007; Alexander et al. 2007). The probability that we are situated in such a void is less than 10^{-12} as can be seen from Fig.5. The probability is exponentially smaller for the larger voids

Table 2. The marginalised cosmological parameters for the various models (with 1σ limits). The 12 parameters in the upper section of the Table are varied by CosmoMC, while those in the lower section are derived quantities. The χ^2 of the fit is given, as is the Akaike information criterion relative to the power-law Λ CDM model.

Parameter	Model		
	Λ CDM power-law	CHDM bump with $n_1 = 12, n_2 = 13$	CHDM bump with n_1, n_2 continuous
$\Omega_b h^2$	$0.02234^{+0.00060}_{-0.00061}$	$0.01674^{+0.00041}_{-0.00047}$	$0.01762^{+0.00095}_{-0.00095}$
$\Omega_c h^2$	$0.1144^{+0.0046}_{-0.0046}$		
θ	$1.0397^{+0.0029}_{-0.0031}$	$1.0311^{+0.0039}_{-0.0039}$	$1.0332^{+0.0048}_{-0.0047}$
τ	$0.0842^{+0.0077}_{-0.0082}$	$0.0721^{+0.0069}_{-0.0075}$	$0.0771^{+0.0073}_{-0.0083}$
$f\nu$		$0.114^{+0.015}_{-0.012}$	$0.085^{+0.015}_{-0.022}$
n_s	$0.961^{+0.014}_{-0.014}$		
$10^4 k_1 / \text{Mpc}^{-1}$		$81.7^{+8.5}_{-8.3}$	87^{+11}_{-11}
$10^4 k_2 / \text{Mpc}^{-1}$		442^{+47}_{-53}	500^{+21}_{-54}
$\ln(10^{10} \mathcal{P}_{\mathcal{R}})$	$3.078^{+0.037}_{-0.037}$		
$\ln(10^{10} \mathcal{P}_{\mathcal{R}}^{(0)})$		$3.294^{+0.031}_{-0.031}$	$3.274^{+0.048}_{-0.048}$
$\ln(10^{10} \mathcal{P}_{\mathcal{R}}^{(1)})$			$3.462^{+0.036}_{-0.036}$
$\ln(10^{10} \mathcal{P}_{\mathcal{R}}^{(2)})$			$3.183^{+0.043}_{-0.041}$
$\Omega_c h^2$		$0.1450^{+0.0079}_{-0.0077}$	$0.156^{+0.012}_{-0.013}$
$\Omega_d h^2$		$0.1634^{+0.0042}_{-0.0045}$	$0.1702^{+0.0073}_{-0.0074}$
h	$0.695^{+0.021}_{-0.021}$	$0.4244^{+0.0052}_{-0.0055}$	$0.4333^{+0.0093}_{-0.0094}$
Age/Gyr	$13.78^{+0.14}_{-0.14}$	$15.36^{+0.20}_{-0.19}$	$15.05^{+0.33}_{-0.32}$
Ω_m	$0.284^{+0.025}_{-0.025}$		
Ω_Λ	$0.716^{+0.025}_{-0.025}$		
σ_8	$0.817^{+0.027}_{-0.027}$	$0.617^{+0.059}_{-0.055}$	$0.700^{+0.098}_{-0.098}$
z_{reion}	$11.0^{+1.4}_{-1.4}$	$13.0^{+2.0}_{-2.0}$	$13.4^{+2.1}_{-2.0}$
Δm_1^2		$0.07495^{+0.00046}_{-0.00046}$	$0.089^{+0.020}_{-0.020}$
Δm_2^2		$0.15133^{+0.00084}_{-0.00084}$	$0.136^{+0.015}_{-0.016}$
$H(t_2 - t_1)$		$1.68^{+0.12}_{-0.13}$	$1.73^{+0.14}_{-0.15}$
χ^2	1339.9	1339.9	1330.2
Δ_{AIC}	0	6.0	-3.7

of Gpc size that have also been considered (Alnes et al. 2006; Garcia-Bellido & Haugboelle 2008a; Clifton et al. 2008).⁶

However before we dismiss the possibility of a local void on these grounds we should also evaluate the probability of

⁶ There is a further constraint on Gpc scale voids from the observed absence of a ‘ y -distortion’ in the spectrum of the CMB (Caldwell & Stebbins 2008) and from the ‘kinetic Sunyaev-Zeldovich’ effect observed for X-ray emitting galaxy clusters (Garcia-Bellido & Haugboelle 2008b). However this has no impact on smaller voids.

voids which have actually been claimed to exist elsewhere in the universe. For example it has been argued that a void with radius $200 - 300 h^{-1} \text{Mpc}$ and an density contrast of $\delta = -0.3$ at $z \sim 1$ can account for the WMAP ‘cold spot’ in a Λ CDM universe (Inoue & Silk 2006). Even if we conservatively take the radius to be $150 h^{-1} \text{Mpc}$ (and the same underdensity), the probability that one or more such voids lie within the volume out to $z = 1$ is only $1.05^{+5.24}_{-0.93} \times 10^{-10}$.

It has been argued that the WMAP cold spot may not be a localized feature (Naselsky et al. 2007) and there may be no matching void in the NVSS radio source cat-

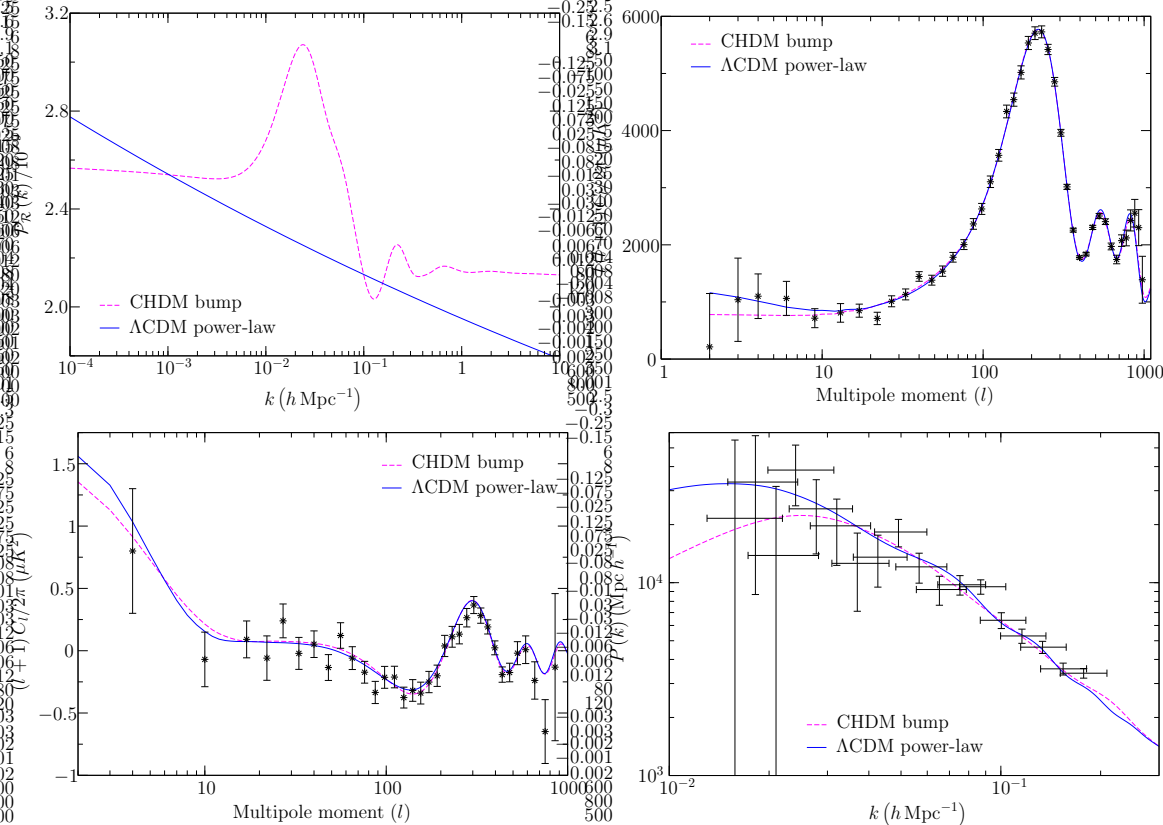


Figure 1. The top left panel shows the primordial perturbation spectrum for the CHDM bump model (with $n_1 = 12$ and $n_2 = 13$) and for the Λ CDM power-law model with $n_s \simeq 0.96$. The top right and bottom left panels show the best-fits for both models to the WMAP-5 TT and TE spectra, while the bottom right panel shows the best-fits to the SDSS galaxy power spectrum.

ologue (Smith & Huterer 2008), however an equally striking anomaly arises if we consider the large number of voids which have been identified in the SDSS LRG survey in a search for the late ISW effect (Granett et al. 2008a,b). These are of angular radius $\sim 4^\circ$ corresponding to a (comoving) radius of $\sim 50 h^{-1} \text{ Mpc}$ and are tabulated as having 1σ , 2σ or 3σ underdensities. These numbers relate to the detection significance (the likelihood of detecting the void by chance out of a Poisson distribution) rather than the likelihood of finding such underdensities in a gaussian field which we have computed in this paper (B. Granett, private communication). Moreover the observed LRGs are biased with regard to the dark matter hence the underdensities in dark matter are likely to be smaller than the quoted values.

However if Granett et al. (2008a,b) have indeed detected the late ISW effect as they assert, we can simply circumvent these uncertainties by requiring that the voids be large enough and/or underdense enough to yield the *observed* CMB temperature decrements. To calculate the late ISW effect we consider the propagation of CMB photons to us from the last scattering surface through an intervening void. The photon temperature change caused by the void is

$$\frac{\Delta T}{T} = -\frac{2}{c^2} \int_{a_{\text{far}}}^{a_{\text{near}}} \frac{d\Phi}{da} da, \quad (23)$$

where a_{far} is the scale factor when the photon crossed the far side of the void and a_{near} is the scale factor when the

photon crossed the near side of the void. The gravitational potential of a void with proper radius r is

$$\Phi = \frac{4\pi G}{3} r^2 \rho_b \delta(a). \quad (24)$$

Here the background density is given by $\rho_b = 3H_0^2 \Omega_m / 8\pi G a^3$ and the density perturbation is given by $\delta(a) = D(a) \delta(a_0)$ where D is the linear growth factor. Hence

$$\frac{\Delta T}{T} = \Omega_m \left(\frac{R}{c/H_0} \right)^2 \left[\frac{D(a_{\text{far}})}{a_{\text{far}}} - \frac{D(a_{\text{near}})}{a_{\text{near}}} \right] \delta. \quad (25)$$

Using this we calculate the expected ISW signal for the 50 highest significance voids in Table 4 of Granett et al. (2008a), employing the concordance Λ CDM cosmology to determine a_{far} and a_{near} for each void from the void redshift measurements. The ISW signal is found to be only $-0.42 \mu\text{K}$ on average if the dark matter underdensities are smaller than the observed underdensities in the LRG counts by the bias factor of 2.2 (taking $\sigma_8 = 0.8$). This is in contrast to the detected mean signal of $-11.3 \mu\text{K}$ which is over 20 times bigger! We must therefore conclude that the void radii and/or underdensities have been significantly underestimated. The void radii can at most be increased by a factor of 1.75 within the quoted uncertainties so the observed signal of $-11.3 \mu\text{K}$ can be matched only if the underdensities are increased by a factor of 5 (implying a bias factor of 0.2). The CMB temperature decrements of such model voids cal-

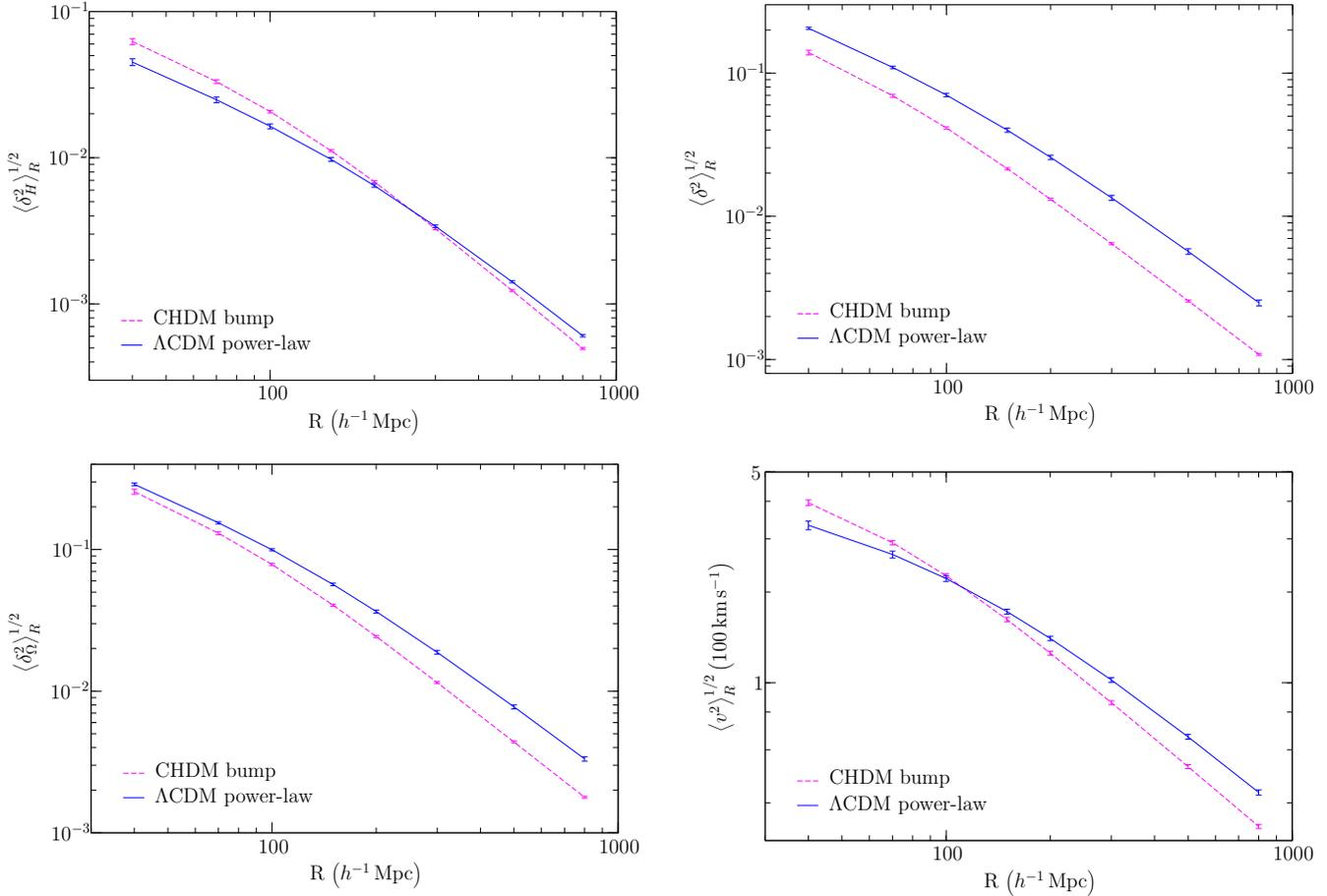


Figure 2. The variation with increasing void radius of the variance of the Hubble parameter, the density contrast, the density parameter and the peculiar velocity for the Λ CDM power-law and CHDM bump models, given the WMAP-5 and SDSS data (with 1σ limits).

culated using eq.(25) are shown in Fig.7 and are (by construction) similar to the actual measurements shown in Fig.2 of Granett et al. (2008b). While such an *underbias* for the observed LRGs may seem implausible, we emphasise that this is the only way in which the temperature decrements observed by Granett et al. (2008a,b) can be accounted for as being due to the late ISW effect.

Fig.7 displays a histogram of the probabilities for finding such voids in the SDSS LRG survey volume ($5 h^{-3} \text{ Gpc}^3$ in the redshift range $0.4 < z < 0.75$). The most improbable void is at $z = 0.672$ — in order to yield the *observed* average CMB temperature decrement it must have a density contrast of -0.72 (quoted galaxy underdensity of -0.316 multiplied by 5/2.2) and a radius of $230 h^{-1} \text{ Mpc}$ (radius derived from the quoted volume of $10^7 h^{-3} \text{ Mpc}^3$ and multiplied by 1.75). The probability of such a void is 1.9×10^{-247} according to our calculations. Although linear theory may not be applicable for such a deep void, it is clear that its existence is in gross conflict with the standard theory of structure formation from *gaussian* primordial density perturbations.

This conclusion is strengthened by the recent detection of very large peculiar velocities on large scales. As seen in Fig.2, the expected variance of the peculiar velocity as calculated by eq.(14) is about 200 km s^{-1} on a scale of $100 h^{-1} \text{ Mpc}$, whereas the measured value is at least 5 times higher,

and the discrepancy is even bigger on larger scales up to 300 Mpc (Kashlinsky et al. 2008).

It is also seen from Fig.5 that if a determination of the Hubble constant is required with say 1% accuracy, then measurements extending out to at least $150 h^{-1} \text{ Mpc}$ must be made to overcome local fluctuations. A similar estimate was made by Li et al. (2008) who noted that the observed variance in measurements of h is in accord, thus consistent with the assumption of a gaussian density field. However the voids observed in the SDSS LRG survey (Granett et al. 2008b) call this assumption into question. In particular whether there is a large local void is then an issue that must be addressed observationally and not dismissed on the grounds that it is inconsistent with gaussian perturbations. The Hubble flow is presently poorly measured in the redshift range $0.1 \lesssim z \lesssim 0.3$ — just where the effects of such a local void would be most apparent (Alexander et al. 2007). Given that dark energy may well be an artifact of such a void, this issue needs urgent attention.

The question of how such voids can have been generated without conflicting with the CMB observations is beyond the scope of the present work. Some suggestions have been made in the context of multi-field inflationary models (Occhionero et al. 1997; DiMarco & Notari 2006; Itzhaki 2008).

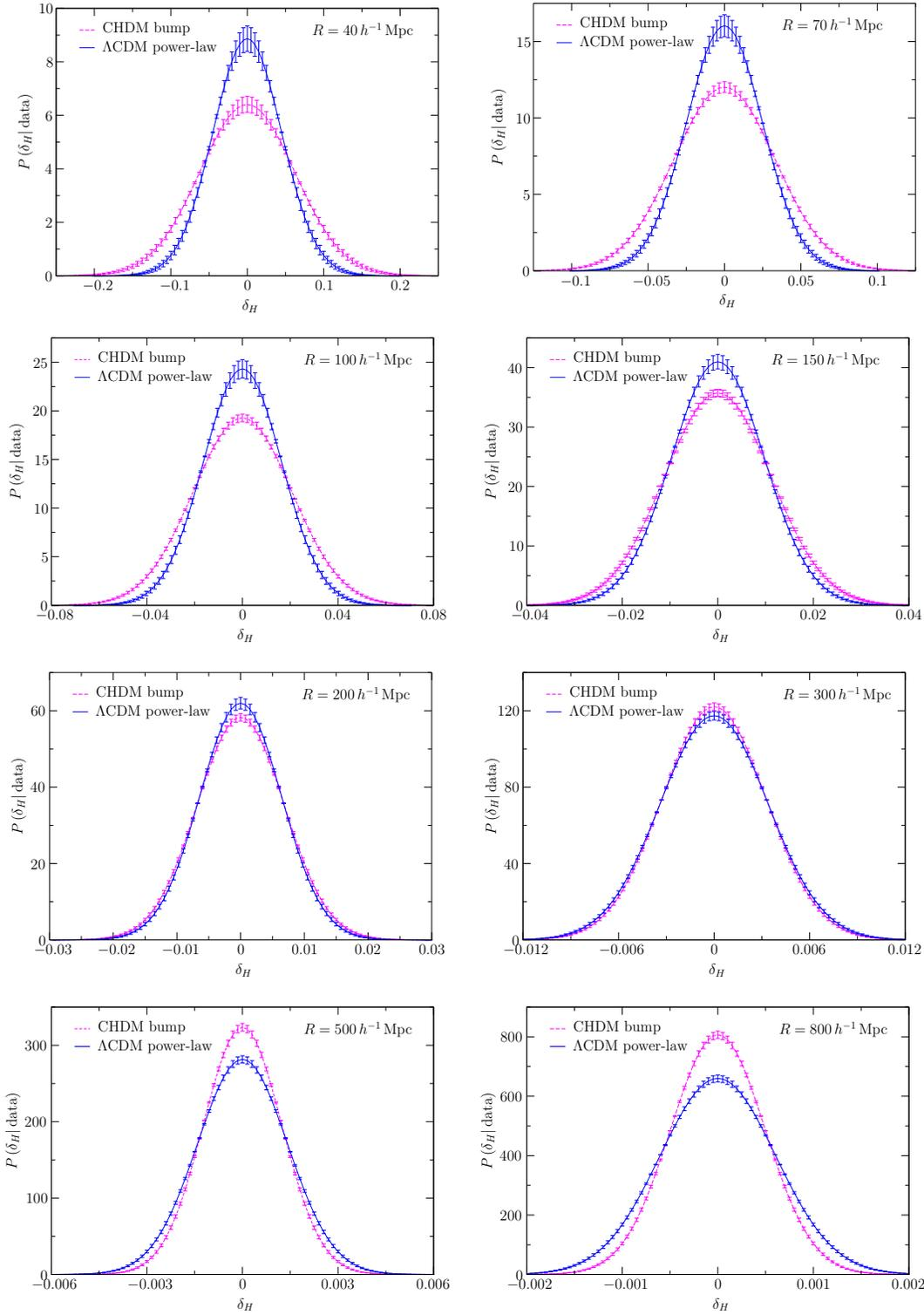


Figure 3. The probability distribution of the Hubble contrast (with 1σ limits), given the WMAP-5 and SDSS data, for the Λ CDM power-law and CHDM bump models, for spherical voids of radius $R = (40, 70, 100, 150, 200, 300, 500, 800) \times h^{-1}$ Mpc.

7 ACKNOWLEDGMENTS

This work was supported by a STFC Senior Fellowship award to S.S. (PPA/C506205/1) and by the EU Marie Curie Network “UniverseNet” (HPRN-CT-2006-035863).

REFERENCES

- Adams J. A., Ross G. G., Sarkar, S., 1997, Nucl. Phys. B, 503, 405
 Akaike, H., 1974, IEEE Trans. Auto. Control, 19, 716
 Alexander S., Biswas T., Notari A., Vaid D., 2007,

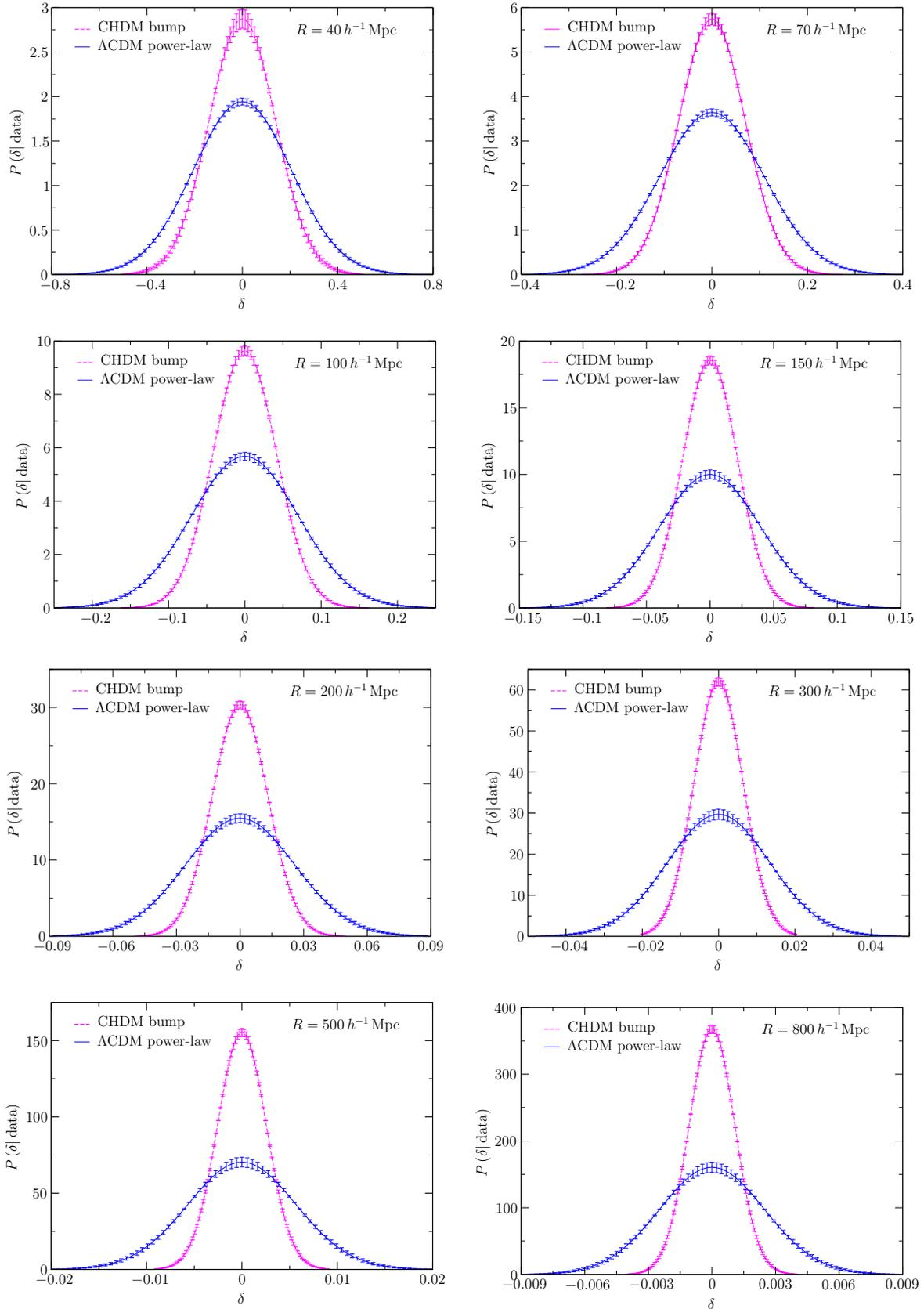


Figure 4. The probability distribution of the density contrast (with 1σ limits), given the WMAP-5 and SDSS data, for the Λ CDM power-law and CHDM bump models, for spherical voids of radius $R = (40, 70, 100, 150, 200, 300, 500, 800) \times h^{-1} \text{ Mpc}$.

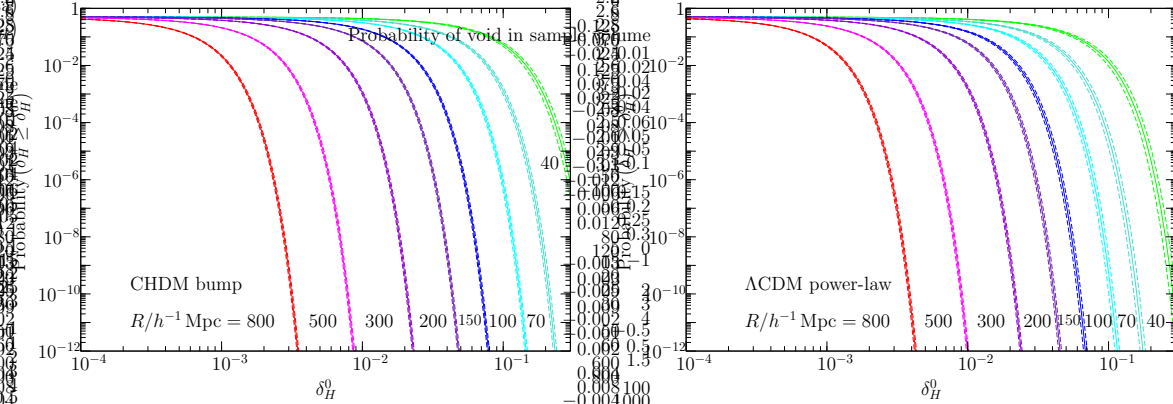


Figure 5. The probability of a fluctuation in the Hubble contrast greater than or equal to a given value δ_H^0 in a sphere of radius R (with 1σ limits), given the WMAP-5 and SDSS data, for the Λ CDM power-law and CHDM bump models for $R = (40, 70, 100, 150, 200, 300, 500, 800) \times h^{-1}$ Mpc.

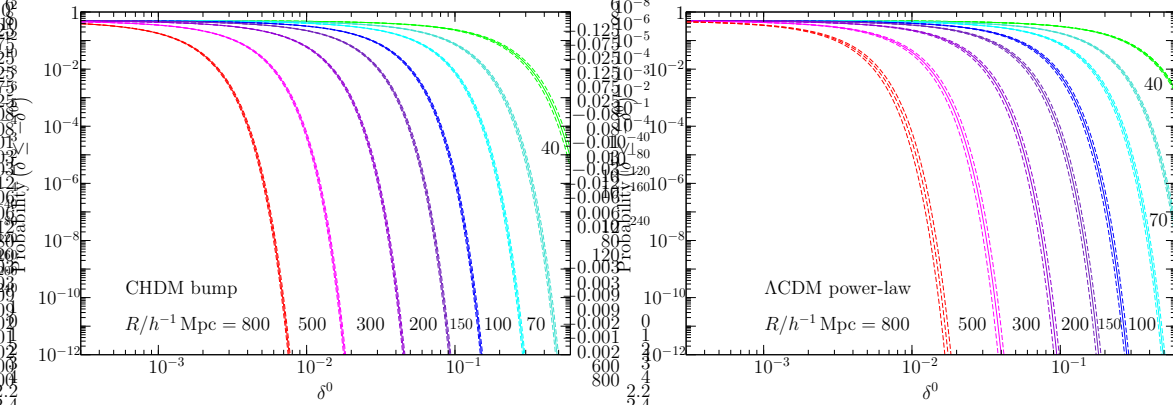


Figure 6. The probability of a fluctuation in the density contrast less than or equal to a given value δ^0 in a sphere of radius R (with 1σ limits), given the WMAP-5 and SDSS data, for the Λ CDM power-law and CHDM bump models for $R = (40, 70, 100, 150, 200, 300, 500, 800) \times h^{-1}$ Mpc.

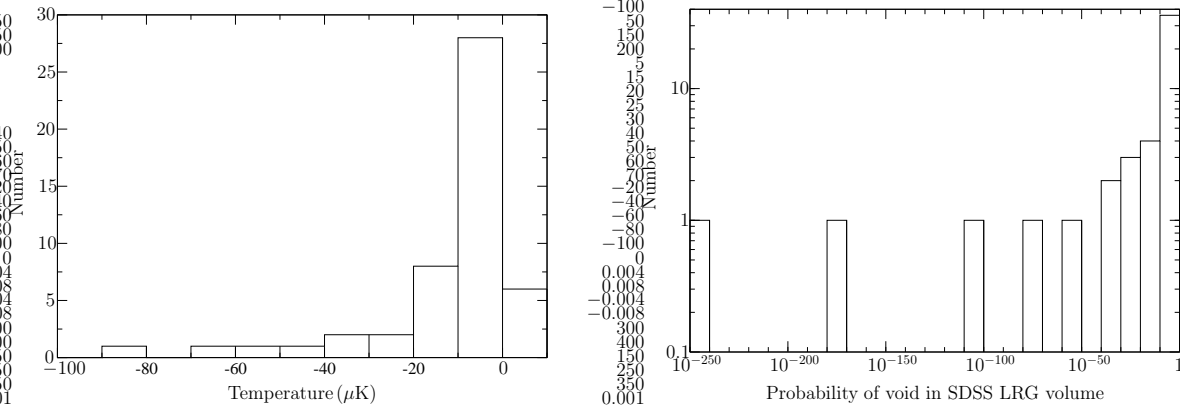


Figure 7. The left panel shows the ISW signals of the 50 voids detected by Granett et al. (2008a), calculated using eq.(25); in order to match the observed average ISW signal of $-11.3 \mu\text{K}$ it has been necessary to increase the void radii by a factor of 1.75 and the underdensities by a factor of 5. The right panel show the probability of such voids occurring in the SDSS LRG survey volume according to the concordance Λ CDM model.

- arXiv:0712.0370 [astro-ph]
 Alnes H., Amarzguioui M., 2007, Phys. Rev. D, 75, 023506
 Alnes H., Amarzguioui M., Gron O., 2006, Phys. Rev. D, 73, 083519
 Arbabi-Bidgoli S., Mueller V., 2002, MNRAS, 332, 205
 Ashoorioon A., Krause A., 2006, arXiv:hep-th/0607001
 Astier P. et al., 2006, A&A, 447, 31
 Bean R., Chen X., Hailu G., Tye S. H., Xu J., 2008, JCAP, 0803, 026
 Behrend J., Brown I. A., Robbers G., 2008, JCAP, 0801, 013
 Benson A. J., Hoyle F., Torres F., Vogeley M. S., 2003, MNRAS, 340, 160
 Biswas T., Notari A., 2008, JCAP, 0806, 021
 Biswas T., Mansouri R., Notari A., 2007, JCAP, 0712, 017
 Blanchard A., Douspis M., Rowan-Robinson M., Sarkar S., 2003, A&A, 412, 35
 Blanchard A., Douspis M., Rowan-Robinson M., Sarkar S., 2006, A&A, 449, 925
 Bolejko K., Wyithe J. S. B., 2009, JCAP, 0902, 020
 Brouzakis N., Tetradis N., 2008, Phys. Lett. B, 665, 344
 Brouzakis N., Tetradis N., Tzavara E., 2008, JCAP, 0804, 008
 Buchert T., 2000, Gen. Rel. Grav., 32, 105
 Buchert T., 2008, Gen. Rel. Grav., 40, 467
 Caldwell R. R., Stebbins A., 2008, Phys. Rev. Lett., 100, 191302
 Celerier M. N., 2000, A&A, 353, 63
 Celerier M. N., 2007, New Adv. Phys., 1, 29
 Chung D. J. H., Kolb E. W., Riotto A., Tkachev I. I., 2000, Phys. Rev. D, 62, 043508
 Chung D. H. J., Romano A. E., 2006, Phys. Rev. D, 74, 103507
 Clarkson C., Bassett B., Lu T. C., 2008, Phys. Rev. Lett., 101, 011301
 Clifton T., Ferreira P. G., Land K., 2008, Phys. Rev. Lett., 101, 131302
 Conroy C. et al., 2005, ApJ, 635, 990
 Contaldi C. R., Hoekstra H., Lewis A., 2003, Phys. Rev. Lett., 90, 221303
 Croton D. J. et al., 2004, MNRAS, 352, 828
 Di Marco F., Notari A., 2006, Phys. Rev. D 73, 063514
 Easter R., Greene B. R., Kinney W. H., Shiu G., 2001, Phys. Rev. D, 64, 103502
 Efstathiou G. et al., 2002, MNRAS, 330, L29
 Eisenstein D. J. et al., 2005, ApJ, 633, 560
 Enqvist K., 2008, Gen. Rel. Grav., 40, 451
 Furlanetto S., Piran T., 2006, MNRAS, 366, 467
 Garcia-Bellido J., Haugboelle T., 2008, JCAP, 0804, 003
 Garcia-Bellido J., and Haugboelle T., 2008, JCAP, 0809, 016
 Garfinkle D., 2006, Class. Quant. Grav., 23, 4811
 Granett B.R., Neyrinck M.C., Szapudi I., 2008, arXiv:0805.2974 [astro-ph].
 Granett B.R., Neyrinck M.C., Szapudi I., 2008, ApJ, 683, L99
 Gong J. O., 2005, JCAP 0507, 015
 Hamilton A. J. S., 2001, MNRAS, 322, 419.
 F. Hoyle and M. S. Vogeley, 2004, ApJ, 607, 751
 Hunt P., Sarkar S., 2004, Phys. Rev. D, 70, 103518
 Hunt P., Sarkar S., 2007, Phys. Rev. D, 76, 123504
 Iguchi H., Nakamura T., Nakao K. i., 2002, Prog. Theor. Phys., 108, 809
 Inoue K.T, Silk J., 2006, ApJ, 648, 23
 Ishibashi A., Wald R. M., 2006, Class. Quant. Grav., 23, 235
 Itzhaki N., 2008, JHEP, 0810, 061
 Kaloper N., Kaplinghat M., 2003, Phys. Rev. D, 68, 123522
 Kashlinsky A., Atrio-Barandela F., Kocevski D., Ebeling H., 2008, ApJ, 686, L49
 Khosravi S., Kourkchi E., Mansouri R., 2009, IJMP D, 18, 1177
 E. Komatsu et al., 2009, ApJS, 180, 330
 Kowalski M., et al., 2008, ApJ, 686, 749
 Lahav, O. Lilje P. B., Primack J. R., Rees J. R., 1991, MNRAS, 251, 128
 Leith B. M., Ng S. C. C., Wiltshire D. L., 2008, ApJ, 672, L91
 Lesgourgues J., 2000, Nucl. Phys. B, 582, 593
 Lewis A., Bridle S., 2002, Phys. Rev. D, 66, 103511
 Lewis A., Challinor A., Lasenby A., 2000, ApJ, 538, 473
 Li N., Seikel M., Schwarz D. J., 2008, Fortsch. Phys., 56, 465
 Little B, Weinberg D. H., 1994, MNRAS, 267, 605
 Mansouri R., 2005, arXiv:astro-ph/0512605
 Marra V., Kolb E. W., Matarrese S., 2008, Phys. Rev. D, 77, 023003
 Marra V., Kolb E. W., Matarrese S., Riotto A., 2007, Phys. Rev. D, 76, 123004
 Mattsson T., 2007, arXiv:0711.4264 [astro-ph]
 Moffat J. W., 2005, JCAP, 0510, 012
 Moffat J. W., 2005, arXiv:astro-ph/0504004
 Moffat J. W., 2006, JCAP, 0605, 001
 Naselsky P. D., Christensen P. R., Coles P., Verkhodanov O., Novikov D., Kim J., 2007, arXiv:0712.1118 [astro-ph]
 Nolta M. R. et al., 2009, ApJS, 180, 296
 Occhionero F., Baccigalupi C., Amendola L., Monastra S., 1997, Phys. Rev. D, 56, 7588
 Padilla N. D., Ceccarelli L., Lambas D. G., 2005, MNRAS, 363, 977
 Paranjape A., Singh T. P., 2008, Phys. Rev. Lett., 101, 181101
 Patiri S. G., Betancort-Rijo J., Prada F., Klypin A., Gottlober S., 2006, MNRAS, 369, 335
 Peebles P. J. E., Principles of physical cosmology, Princeton Univ. Press, Princeton, NJ
 Peebles P. J. E., Ratra B., 2003, RMP, 75, 559
 Perlmutter S. et al., 1999, ApJ, 517, 565
 Rasanen S., 2008, JCAP 0804, 026
 Riess A. G. et al., 1998, AJ, 116, 1009
 Riess A. G. et al., 2004, ApJ, 607, 665
 Rudnick L., Brown S., Williams L. R., 2007, ApJ, 671, 40
 Sarkar S., 2008, Gen. Rel. Grav., 40, 269
 Schmidt J. D., Ryden B. S., Melott A. L., 2001, ApJ, 546, 609
 Shandarin S., Feldman H. A., Heitmann K., Habib S., 2006, MNRAS, 367, 1629
 Sheth R. K., van de Weygaert R., 2004, MNRAS, 350, 517
 Shi X., Widrow L. M., Dursi L. J., 1996, MNRAS, 281, 565
 Smith R. E. et al., 2003, MNRAS, 341, 1311
 Smith K. M., Huterer D., 2008, arXiv:0805.2751 [astro-ph].
 Spergel D. N. et al., 2003, ApJS, 148, 175
 Spergel D. N. et al., ApJS, 170, 377 (2007).

- Tegmark M. et al., 2004, ApJ, 606, 702
Tikhonov A. V., 2006, Astron. Lett., 32, 727
Tikhonov A. V., 2007, Astron. Lett., 33, 499
Tinker J. L., Conroy C., Norberg P., Patiri S. G., Weinberg D. H., Warren M. S., 2004, ApJ, 686, 53
Tomita K., 2000, ApJ, 529, 26
Tomita K., 2001, Prog. Theor. Phys., 105, 419
Tomita K., 2001, MNRAS, 326, 287
Tomita K., 2001, Prog. Theor. Phys., 106, 929
Tomita K., 2003, ApJ, 584, 580
Turner E. L., Cen R. y., Ostriker J. P., 1992, AJ, 103, 1427
Uzan J. P., Clarkson C., Ellis G. F. R., 2008, Phys. Rev. Lett., 100, 191303
Vanderveld R. A., Flanagan E. E., Wasserman I., 2006, Phys. Rev. D, 74, 023506
Vanderveld R. A., Flanagan E. E., Wasserman I., 2007, Phys. Rev. D, 76, 083504
von Benda-Beckmann A. M., Mueller V., 2007, arXiv:0710.2783 [astro-ph].
Wang X., Feng B., Li M., Chen X. L., Zhang X., 2005, IJMP D, 14, 1347
Wang Y., Spergel D. N., Turner E. L., 1998, ApJ, 498, 1
Watkins R., Feldman H. A., Hudson M. J., 2009, MNRAS, 392, 743
Weinberg S., 1989, Rev. Mod. Phys., 61, 1
Wetterich C., 2003, Phys. Rev. D, 67, 043513
Wiltshire D. L., 2007, Phys. Rev. Lett., 99, 251101
Wood-Vasey W. M et al., 2007, ApJ, 666, 694